

Lattice dynamics of rare-gas overlayers on smooth surfaces

Burl Hall and D. L. Mills

Department of Physics, University of California, Irvine, California 92715

J. E. Black

Department of Physics, Brock University, Saint Catharines, Ontario, Canada L2S 3A1

(Received 15 February 1985)

We discuss the lattice dynamics of rare-gas overlayers on metal surfaces, with attention to monolayers, bilayers, and trilayers on the Ag(111) surface. For this system, the adsorbate overlayers are incommensurate with the metal substrate. Our interest is in the role of the interaction between the motions of the atoms in the adlayers and those of substrate atoms. In certain regions of the two-dimensional Brillouin zone, the adlayer phonon dispersion curves (calculated with the substrate atoms held in fixed position) overlap the bulk phonon bands of the semi-infinite substrate. A consequence is that when excited, the adlayer phonon may decay by emitting phonons into the substrate. They thus become leaky modes. Also, the adlayer modes may hybridize with the Rayleigh surface phonon on the substrate, to produce anomalous dispersion near those wave vectors where crossover occurs. For Ar, Kr, and Xe overlayers on models of Ag(111), we explore these phenomena through calculations of the phonon spectral density functions probed in inelastic He-surface scattering experiments.

I. INTRODUCTION

When rare-gas atoms are adsorbed on crystal surfaces, they may form ordered overlayers. Often these are incommensurate with the underlying substrate. There are two limits to the problem. On highly corrugated surfaces, with graphite the most studied example,¹ the depth of the periodic potential felt by an atom adsorbed is comparable to the strength of the lateral interactions between the adsorbates. With increasing coverage, one realizes a commensurate-incommensurate transition, and in fact at all coverages, interaction of the adsorbate layer with the corrugated substrate potential is an important influence.

On the other hand, close-packed metal surfaces are extraordinarily smooth, to adsorbates which are physisorbed. Such surfaces look so smooth to the adsorbate that the overlayers form two-dimensional lattices incommensurate with the substrate, with lattice constant quite close to (but surely a bit different than) that predicted from a lattice statics calculation based on gas-phase potentials. Rare-gas monolayers on Ag(111), an extraordinary smooth surface, have been studied extensively by the authors in Ref. 2. These authors argue that in their data, nearly all of which refer to static properties of the overlayer, there is no evidence of interaction of the adlayers with the substrate. We have recently participated in an analysis of data on phonon dispersion curves for rare-gas monolayers, bilayers, and the layers adsorbed on Ag(111), and again the data provides no evidence of interaction between these modes, and the phonons of the substrate.³ Similar conclusions follow from the early work of Mason and Williams,⁴ who studied Xe monolayers on Cu(100) by inelastic He scattering.

It would be extremely intriguing to see explicit evidence of the interaction between rare-gas overlayers and the sub-

strate, for rare-gas overlayers on very smooth surfaces such as Ag(111). We believe that the study of surface phonons should allow this to be done since, as we shall appreciate shortly, the frequencies of the adlayer phonons coincide with those of the substrate phonons, in appropriate portions of the two-dimensional Brillouin zone. One should be able to see clear evidence of interaction effects between an adlayer surface phonon of given frequency and wave vector Q_{\parallel} parallel to the surface, and a substrate surface phonon of the same frequency and wave vector, even if this coupling is rather weak. Observation of such interactions might be able to improve our understanding of how the substrate influences the incommensurate overlayer in the limit where the substrate surface is very smooth.

The failure to observe interactions between the substrate modes and phonons of the adlayers may lie in the fact that the regions of the two-dimensional Brillouin zone where the strongest coupling effects are expected have not been explored with sufficient resolution and detail. Theoretical studies may then provide useful guidance to the experimentalist. This paper is devoted to such analyses.

Since the overlayers of interest are incommensurate with the substrate, with lattice constant determined primarily by lateral interactions between adsorbates,^{2,3} a full discussion of the dynamics of the coupled adlayer-substrate system will be formidable. We wish not to address this question in full at this early stage, therefore, we resort to the use of two models each of which contain the ingredient central to the problem, but which may be explored in full detail without confronting the very intriguing but difficult question of incommensurability.

The points we wish to emphasize here may be illustrated by considering a monolayer of rare-gas adsorbate on

the Ag(111) surface. Data reported earlier^{3,4} show that a dispersionless surface mode is associated with the adlayer, if we consider adatom motions normal to the surface. In theory, such a dispersionless surface mode follows from any model which does not consider the influence of motions of the substrate atoms [hence, the only role of the substrate is to provide the physisorption potential $V(z)$, which binds the adsorbates to the surface], and which assumes lateral interactions between the rare-gas adatoms to have central-force character.

In a very schematic fashion, we illustrate the normal mode structure of the adlayer-substrate system in Fig. 1. For convenience, we assume that the lattice constant in the two directions parallel to the surface is the same for each system. At the zone boundary \bar{M} (the direction $\bar{\Gamma}-\bar{M}$ was the subject of study in Ref. 3), the substrate phonon frequencies are substantially above those of the adlayer, and the influence of substrate-adlayer coupling is expected to be small. But as we move toward $\bar{\Gamma}$, the dispersionless adlayer mode necessarily crosses the dispersion curve of the Rayleigh surface phonon. We expect hybridization between the adlayer mode and the Rayleigh wave. The calculations below show, for the models explored, that the coupling introduces anomalous dispersion into the adlayer mode.

As we proceed close to $\bar{\Gamma}$, the adlayer mode overlaps the acoustical-phonon continuum of the substrate. In this regime of the two-dimensional Brillouin zone, if the adlayer is excited, the energy stored in the motion of the adatoms may be radiated off into the substrate, in the form of bulk transverse or longitudinal phonons.⁵ The monolayer mode is thus no longer a true eigenmode of the system, but acquires a finite lifetime by virtue of this radiative decay process. This is true even in the harmonic approximation of lattice dynamics. As long as many cycles of oscillations are required for the energy to be radiated in this fashion, there is a strong resonant response of the system very close to the frequency of the adlayer mode, calculated in the rigid substrate limit. One refers to this as a surface resonance mode; for an oxygen overlayer on the Ni(111) surface, we have presented a detailed discussion of the properties of such resonance modes, although in that case the origin of the surface resonance modes differs substantially from the present case.⁶ In this paper we present calculations of the width of the resonance modes of the rare-gas overlayers as a function of their wave vector, for argon, krypton, and xenon overlayers on Ag(111).

The two models we consider are the following. The justification for the first is that for the particular systems of interest, the crossover between the Rayleigh wave and monolayer perpendicular mode lies quite close to $\bar{\Gamma}$. The Rayleigh waves of interest (and also the bulk phonons in the substrate continuum) thus have wavelengths rather long compared to the substrate lattice constant. The response of the substrate to the adlayer atom motions may thus be described by the theory of elasticity. The first model is then that of rare-gas monolayers, bilayers, and trilayers coupled to the surface of a perfectly smooth, semi-infinite elastic continuum. We may extrapolate the predictions of such a model to short wavelengths in the spirit of the Debye model, but we recognize that near the

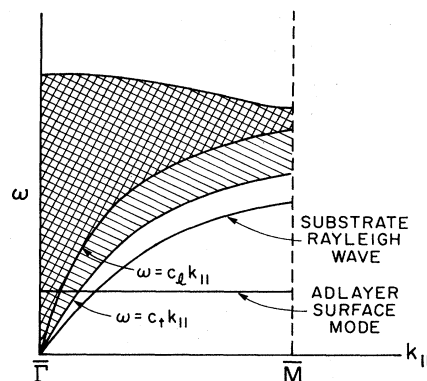


FIG. 1. A schematic representation of the normal mode structure of the adlayer-substrate system. We show a dispersionless adlayer surface mode, the Rayleigh surface phonon of the substrate, and the bulk surface phonons of the substrate projected onto the two-dimensional surface Brillouin zone.

zone boundary the predictions have semiquantitative validity only. The second model is based on the observation that the xenon monolayer is almost commensurate with the substrate; the adlayer-substrate lattice-constant ratio is very close to $\frac{3}{2}$. Thus, we explore, with the slab method, the lattice dynamics of such a commensurate system. When the results of the two model calculations are compared in the appropriate manner, the same physical features are seen to be present in each, although, as expected, there are quantitative differences likely due to the fact that we can explore only rather thin slabs, for reasons discussed below.

These calculations outline the principal ways in which coupling between adlayer and substrate motions may influence the lattice dynamics of rare-gas overlayers, which possess very-low-frequency normal modes. We believe the predictions to be accurate at the semiquantitative level. If these effects can be observed, deviations from the picture discussed here may lead to insight into the role of incommensurability.

The discussion above has placed emphasis on the rare-gas overlayers on Ag(111) which, as we have remarked, is a very smooth surface. Mason and Williams⁷ have also explored the vibrations of Kr and Xe monolayers on the Ag(110) surface, which is highly corrugated. These data also show dispersionless behavior for the adsorbate vibration mode polarized normal to the surface. Possibly this is because the adsorbates reside within the troughs present on this surface, with identical binding site for each, and there are then only weak couplings between them in the direction normal to the troughs. The physics of the adsorbate layers on the (110) surface is, quite likely different than on the very smooth metal (100) surfaces.

This paper is organized as follows. Section II sets up the theory of the coupling of adlayers to elastic continua, and Sec. III presents and discusses our results for both models.

II. INTERACTION OF ADLAYERS WITH SUBSTRATE PHONONS; SEMI-INFINITE ELASTIC CONTINUUM MODEL

Of the two models discussed in Sec. I, one of them (the slab method) requires little explicit discussion. In this section, we outline the interaction of an ordered overlayer (or multilayer film) with a substrate viewed as a semi-infinite elastic continuum.

The basic physical picture is illustrated in Fig. 2. We have one (or more) periodic overlayers of adatoms, each of mass M_A . Each layer will be assumed hexagonal in the subsequent discussion, and there are lateral interactions within each layer, and between adlayers in the multilayer films we shall consider. The atoms in the adlayer closest to the substrate are each attached to a point immediately below by means of a harmonic spring of spring constant k_0 . All such springs are attached to points located in a plane which lies the distance z_0 below the surface of the substrate, viewed once again as a semi-infinite elastic continuum. In the end, we shall let $z_0 \rightarrow 0$, but for certain technical reasons we keep this quantity finite for a while.

All of the discussion will be based on the harmonic approximation of lattice dynamics, so that there is no difference between the equations of motion in a quantum-mechanical treatment of the problem, or a classical treatment. In the end, the spectral density functions we calculate may be viewed as describing the fully-quantum-mechanical system.

We choose to employ a Lagrangian approach, and write the Lagrangian in the form

$$L = L_A + L_S + L_I, \quad (2.1)$$

with L_A providing a description of the adsorbate overlayers, L_S the substrate, and L_I the interactions between the two. The α th Cartesian coordinate of the substrate displacement will be denoted by $u_\alpha(\mathbf{x}, t)$, and that of the adsorbate atom located at $l = l_{||} + \hat{z}l_z$ is $w_\alpha(l_{||}, l_z; t)$. Here, \hat{z} is a unit vector normal to the surface while $l_{||}$ is the projection of l on a plane parallel to the surface.

If M_A is the mass of the adsorbate atoms, we have

$$L_A = \frac{1}{2} M_A \sum_{l_{||}, l_z} \sum_{\alpha} [\dot{w}_\alpha(l_{||}, l_z)]^2 - \frac{1}{2} \sum_{l_{||}, l_z} \sum_{\alpha, \beta} w_\alpha(l_{||}, l_z) \Phi_{\alpha\beta}(l_{||}, l_z; l'_{||}, l'_z) w_\beta(l'_{||}, l'_z) \quad (2.2)$$

and if ρ is the mass density of the substrate, we have

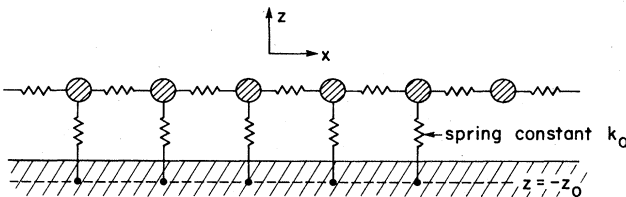


FIG. 2. Our model of a periodic adlayer of atoms, mass M_A , coupled to a semi-infinite elastic substrate by springs of spring constant k_0 .

$$L_S = \int_{z \leq 0} d^3x \left[\frac{\rho}{2} \sum_{\alpha} \dot{u}_\alpha(\mathbf{x}, t) - V(\{\partial u_\alpha / \partial x_\beta\}) \right], \quad (2.3)$$

where V is the potential energy of the deformed substrate; we shall not require the precise form of V , except to note that it is a functional of the spatial derivatives $\partial u_\alpha / \partial x_\beta$ of the displacement.⁸

Finally, for L_I , the physical picture illustrated in Fig. 2 suggests that we choose

$$L_I = -\frac{1}{2} k_0 \sum_{l_{||}} [w_z(l_{||}, 0) - u_z(l_{||}, -z_0)]^2, \quad (2.4)$$

where $l_z = 0$ refers to the layer of adsorbate atoms closest to the substrate, and $\mathbf{u}(\mathbf{x})$ is written $\mathbf{u}(l_{||}, z)$ when convenient. Note that Eq. (2.4) may also be written as an integral over the half-space ($z \leq 0$) occupied by the substrate

$$L_I = -\frac{1}{2} k_0 \sum_{l_{||}} \int_{z < 0} d^3x [w_z(l_{||}, 0) - u_z(\mathbf{x}_{||}, z)]^2 \times \delta(\mathbf{x}_{||} - l_{||}) \delta(z + z_0). \quad (2.5)$$

It is straightforward to generate the equations of motion for the various displacements:

$$\ddot{w}_\alpha(l_{||}, l_z) + \frac{1}{M_A} \sum_{l'_{||}, l'_z} \sum_{\beta} \Phi_{\alpha\beta}(l_{||}, l_z; l'_{||}, l'_z) w_\beta(l'_{||}, l'_z) = -\delta_{l_z 0} \delta_{\alpha z} \frac{k_0}{M_A} [w_z(l_{||}, 0) - u_z(l_{||}, -z_0)], \quad (2.6)$$

while

$$\rho \ddot{u}_\alpha - \sum_{\beta} \frac{\partial}{\partial x_\beta} T_{\alpha\beta} = \delta_{\alpha\beta} \delta(z + z_0) k_0 \times \sum_{l_{||}} [w_z(l_{||}, 0) - u_z(l_{||}, -z_0)] \delta(\mathbf{x}_{||} - l_{||}). \quad (2.7)$$

Here, $T_{\alpha\beta} = \partial V / \partial (\partial u_\alpha / \partial x_\beta)$ is the stress tensor of elasticity theory.⁸ To find the normal modes of the adsorbate-substrate system, one solves Eqs. (2.6) and (2.7) in the manner described below, subject to the boundary condition

$$T_{z\beta} |_{z=0} = 0 \quad (2.8)$$

for $\beta = x, y$, and z .

The innermost layer of the adsorbate structure is assumed to be a Bravais lattice, with one site located at the origin of the coordinate system, $l_{||} = 0$. We seek solutions with a wavelike variation parallel to the surface, with wave vector $\mathbf{Q}_{||}$ which lies within the two-dimensional Brillouin zone parallel to the surface:

$$w_z(l_{||}, l_z) \equiv w_z(\mathbf{0}, l_z) e^{i\mathbf{Q}_{||} \cdot l_{||}}, \quad (2.9a)$$

$$u_z(l_{||}, -z_0) = u_z(\mathbf{0}, -z_0) e^{i\mathbf{Q}_{||} \cdot l_{||}}. \quad (2.9b)$$

We define

$$\Delta = w_z(\mathbf{0}, 0) - u_z(\mathbf{0}, -z_0), \quad (2.10)$$

and use the identity

$$\sum_{l_{||}} e^{i\mathbf{Q}_{||}\cdot l_{||}} \delta(\mathbf{x}_{||} - l_{||}) = \frac{1}{A_0} \sum_{\mathbf{G}_{||}} e^{i(\mathbf{Q}_{||} + \mathbf{G}_{||})\cdot \mathbf{x}_{||}}, \quad (2.11)$$

where A_0 is the area of the two-dimensional unit cell of the adsorbate layer and $\{\mathbf{G}_{||}\}$ is the set of reciprocal lattice vectors that characterize it. Then Eq. (2.7) becomes, after assuming that all quantities have the time variation $\exp(-i\Omega t)$,

$$\rho\Omega^2 u_\alpha(\mathbf{x}) + \sum_{\beta} \frac{\partial T_{\alpha\beta}}{\partial x_\beta} = -\delta_{\alpha z} \delta(z+z_0) \frac{k_0 \Delta}{A_0} \sum_{\mathbf{G}_{||}} e^{i(\mathbf{Q}_{||} + \mathbf{G}_{||})\cdot \mathbf{x}_{||}}. \quad (2.12)$$

In Eq. (2.12), combined with the boundary condition in Eq. (2.8), we have a semi-infinite elastic substrate, driven by a force applied at the plane $z = -z_0$, with frequency Ω . If $\mathbf{Q}_{||}$ is the wave vector of the normal mode of the adsorbate layer, then the applied force has the spatial variation $\exp(i\mathbf{Q}_{||}\cdot \mathbf{x}_{||})$. The terms with $\mathbf{G}_{||} \neq 0$ in Eq. (2.12) have their physical origin in the particular physical picture displayed in Fig. 2, namely, the spring from the adsorbate atom down to the substrate is anchored to the geometrical point directly below the adsorbate atom. With the substrate driven at a periodic array of geometrical points in a plane, a phonon of wave vector $\mathbf{Q}_{||}$ in the adsorbate layer excites not only motion with the same wave vector in the substrate, but in addition it excites short-wavelength responses with the spatial variation $\exp[i(\mathbf{Q}_{||} + \mathbf{G}_{||})\cdot \mathbf{x}_{||}]$. As indicated in Sec. I, our primary interest lies in values of $\mathbf{Q}_{||}$ near the center of the two-dimensional Brillouin zone Γ , and coupling of adsorbate motions to those modes of the substrate in resonance with the adsorbate modes. These substrate motions are described by the terms with $\mathbf{G}_{||} = 0$ in Eq. (2.12). We thus discard the terms with $\mathbf{G}_{||} \neq 0$ in Eq. (2.12) and replace the equation of motion by

$$\rho\Omega^2 u_\alpha(\mathbf{x}) + \sum_{\beta} \frac{\partial T_{\alpha\beta}}{\partial x_\beta} = -\delta_{\alpha z} \delta(z+z_0) \frac{k_0 \Delta}{A_0} e^{i\mathbf{Q}_{||}\cdot \mathbf{x}_{||}}. \quad (2.13)$$

The expression in Eq. (2.13) also follows if we assume the adsorbate atom senses not only the motion of the one point in the substrate just below it, but responds to the average displacement of the unit cell just below it. In this picture, our instructions are to average the coupling term over the unit cell, and $\langle e^{i\mathbf{G}_{||}\cdot \mathbf{x}_{||}} \rangle = \delta_{\mathbf{G}_{||}, 0}$. The form of the terms with $\mathbf{G}_{||} \neq 0$ in Eq. (2.12) is sensitive to the microscopic details of the model employed for coupling the adsorbate layer to the substrate, and cannot be obtained uniquely from a continuum model of the substrate, which cannot provide a reliable description of its short-wavelength response. But the $\mathbf{G}_{||} = 0$ term gives a rigorous account of the coupling of the adsorbate overlayer to the long-wavelength ($\mathbf{Q}_{||} \approx 0$) modes of the substrate, and it is these couplings that we focus our attention on here. As we shall see, the conclusions we reach with our continuum model based on Eq. (2.13) are in accord with those deduced from the fully microscopic slab calculation mentioned in Sec. I, so a comparison between the

two model calculations provides us with confidence in the procedure just described.

We now proceed as follows. When the Bloch forms given in Eq. (2.9a) are inserted into Eq. (2.6), then we find

$$\Omega^2 w_\alpha(\mathbf{0}, l_z) - \sum_{l'_z, \beta} \left[d_{\alpha\beta}(\mathbf{Q}_{||}; l_z l'_z) + \delta_{\alpha z} \delta_{l_z, 0} \frac{k_0}{M_A} \right] w_\alpha(\mathbf{0}, l_z) = -\frac{k_0}{M_A} \delta_{l_z, 0} \delta_{\alpha z} u_z(\mathbf{0}, -z_0), \quad (2.14)$$

where

$$d_{\alpha\beta}(\mathbf{Q}_{||}; l_z l'_z) = \frac{1}{M_A} \sum_{l_{||}} \Phi_{\alpha\beta}(l_{||}, l_z; l_{||}, l'_z) e^{-i\mathbf{Q}_{||}\cdot(l_{||} - l'_{||})}. \quad (2.15)$$

If we discard the right-hand side of Eq. (2.14), then we have a limiting form of the model which formed the basis of our earlier analysis³ of the vibrational motion of rare-gas monolayers, bilayers, and trilayers on Ag(111). The matrix $d_{\alpha\beta}(\mathbf{Q}_{||}; l_z l'_z)$ describes the influence of lateral interactions between the adsorbates on the phonon spectrum of the overlayer, and the term proportional to k_0/M_A describes the coupling of the overlayer with a perfectly rigid, perfectly smooth substrate whose only role is envisioned as providing a harmonic restoring force when an atom in the innermost layer engages in vertical motion about its equilibrium position. The constant k_0 may be generated from a phenomenological physisorption potential such as that provided by Vidali, Cole, and Klein,⁹ as discussed earlier.³

When the term on the right-hand side of Eq. (2.14) is retained, then Eq. (2.14) in combination with Eq. (2.12) describes coupled motion of the adsorbate-substrate system. By solving Eq. (2.12) with the boundary conditions in Eq. (2.14) applied, we shall find that $u_z(\mathbf{0}, -z_0)$ is directly proportional to $w_z(\mathbf{0}, 0)$. We write this relation in the form

$$u_z(\mathbf{0}, -z_0) = \frac{k_0}{M_A} S(\mathbf{Q}_{||}, \Omega) w_z(\mathbf{0}, 0), \quad (2.16)$$

and then Eq. (2.14) assumes the form

$$\Omega^2 w_\alpha(\mathbf{0}, l_z) - \sum_{l'_z, \beta} \left[d_{\alpha\beta}(\mathbf{Q}_{||}; l_z l'_z) + \delta_{\alpha z} \delta_{l_z, 0} \frac{\tilde{k}_0(\mathbf{Q}_{||}, \Omega)}{M_A} \right] w_\alpha(\mathbf{0}, l_z) = 0 \quad (2.17)$$

where

$$\tilde{k}_0(\mathbf{Q}_{||}, \Omega) = k_0 [1 - S(\mathbf{Q}_{||}, \Omega)]. \quad (2.18)$$

We see that inclusion of the dynamical response of the substrate may be incorporated by simply renormalizing the force constant which couples the innermost adsorbate

layer to the substrate. Of course, this renormalization effect depends on both frequency and wave vector, as indicated, so we no longer have a straightforward eigenvalue problem to explore. In earlier work,^{6,10} we have found it most illuminating to construct spectral density functions which, in essence, provide one with the frequency spectrum of selected atomic motions in or near the surface. These spectral density functions may be calculated straightforwardly from an elementary modification of Eq. (2.17). We discuss the definition of the spectral density functions in Sec. III, and the means of calculating them from Eq. (2.17).

Our remaining task is the construction of $S(\mathbf{Q}_{||}, \Omega)$. In principal, we should proceed by treating the substrate as a cubic material with a (111) surface. In fact, the form of $S(\mathbf{Q}_{||}, \Omega)$ is quite simple if we treat the substrate as an isotropic elastic continuum characterized by the velocities c_l and c_t of longitudinal and transverse sound, while an analysis of the lower symmetry cubic material is very complex simply from the algebraic point of view. We thus choose to confine our attention to the case where the substrate is approximated as an isotropic continuum.

For the isotropic continuum driven by a force normal to the surface (parallel to \hat{z}), and with the spatial variation $\exp(i\mathbf{Q}_{||} \cdot \mathbf{x}_{||})$, the displacement \mathbf{u} lies within the sagittal plane, i.e., the plane which contains both \hat{z} and $\mathbf{Q}_{||}$. We may then choose $\mathbf{Q}_{||}$ parallel to the x axis, without loss of generality, and a consequence is that \mathbf{u} lies in the x - z plane. If $w \Lambda_0 = k_0 \Delta / A_0$, and assume all quantities exhibit the $\exp(i\mathbf{Q}_{||} \cdot \mathbf{x}_{||})$ spatial variation, then Eq. (2.13) yields a set of two coupled equations which assume the form

$$(c_l^2 Q_{||}^2 - \Omega^2) u_z - c_l^2 \frac{\partial^2 u_z}{\partial z^2} - i Q_{||} (c_l^2 - c_t^2) \frac{\partial u_x}{\partial z} = \Lambda_0 \delta(z + z_0) \quad (2.19a)$$

$$(c_l^2 Q_{||}^2 - \Omega^2) u_x - c_t^2 \frac{\partial^2 u_x}{\partial z^2} - i Q_{||} (c_l^2 - c_t^2) \frac{\partial u_z}{\partial z} = 0, \quad (2.19b)$$

while the stress-free boundary conditions at $z=0$ impose the requirements

$$\left. \left[\frac{\partial u_x}{\partial z} + i Q_{||} u_z \right] \right|_{z=0} = 0, \quad (2.20a)$$

$$\left. \left[c_l^2 \frac{\partial u_z}{\partial z} + i (c_l^2 - 2c_t^2) Q_{||} u_x \right] \right|_{z=0} = 0. \quad (2.20b)$$

One proceeds by solving the homogeneous version of the differential equations in the regime $-\infty \leq z < -z_0$, and joining the solutions across $z = -z_0$ so that the δ -function singularity is generated on the right-hand side of Eq. (2.19a) after suitable differentiations are performed. The matching conditions are that each component of displacement be continuous:

$$u_x(z_0^-) = u_x(z_0^+), \quad (2.21a)$$

$$u_z(z_0^-) = u_z(z_0^+), \quad (2.21b)$$

and from the structure of the differential equation, one obtains the additional requirements

$$\left[\frac{\partial u_x}{\partial z} \right]_{z_0^-} = \left[\frac{\partial u_x}{\partial z} \right]_{z_0^+} \quad (2.22a)$$

and

$$\left[\frac{\partial u_z}{\partial z} \right]_{z_0^-} - \left[\frac{\partial u_z}{\partial z} \right]_{z_0^+} = \frac{1}{c_l^2} \Lambda_0. \quad (2.22b)$$

It is straightforward to see that the homogeneous versions of Eqs. (2.19) have solutions proportional to $\exp(\pm \alpha_l z)$ and also $\exp(\pm \alpha_t z)$, where

$$\alpha_l = \left[Q_{||}^2 - \frac{1}{c_l^2} (\Omega + i\eta)^2 \right]^{1/2}, \quad \text{Re}(\alpha_l) > 0 \quad (2.23a)$$

and

$$\alpha_t = \left[Q_{||}^2 - \frac{1}{c_t^2} (\Omega + i\eta)^2 \right]^{1/2}, \quad \text{Re}(\alpha_t) > 0. \quad (2.23b)$$

Here, η is a positive infinitesimal quantity; we insert it to ensure that we always choose the square root with a positive real part both when $Q_{||} < \Omega/c_{l,t}$ and also when $Q_{||} > \Omega/c_{l,t}$. The limit $\eta \rightarrow 0$ is implied, although we shall appreciate that it is most useful to retain small positive values of η when numerical calculations are performed.

The most general solution of the homogeneous version of Eqs. (2.19) may then be written

$$u_z = A_+^{(l)} e^{+\alpha_l z} + A_-^{(l)} e^{-\alpha_l z} + A_+^{(t)} e^{+\alpha_t z} + A_-^{(t)} e^{-\alpha_t z} \quad (2.24a)$$

and then

$$u_x = i \frac{Q_{||}}{\alpha_l} (A_+^{(l)} e^{+\alpha_l z} - A_-^{(l)} e^{-\alpha_l z}) + i \frac{\alpha_t}{Q_{||}} (A_+^{(t)} e^{+\alpha_t z} - A_-^{(t)} e^{-\alpha_t z}). \quad (2.24b)$$

In the region $-\infty \leq z \leq -z_0$, we choose a solution with $A_-^{(l)} = A_-^{(t)} \equiv 0$ so that the displacement fields vanish as $z \rightarrow -\infty$, while in the regime $-z_0 \leq z \leq 0$ the full solution is employed. We thus have six unknown constants; the two stress-free boundary conditions and the four matching conditions at $z = -z_0$ are sufficient to determine these. After some algebra, with z_0 fixed and nonzero, we may calculate $u_z(\mathbf{x}_{||}, z)$ at $(\mathbf{x}_{||} = \mathbf{0}, z = 0)$, then let $z_0 \rightarrow 0$ to form the quantity $u_z(\mathbf{0}, 0)$ of our earlier discussion. We find a rather simple result:

$$u_z(\mathbf{0}, 0) = \frac{\Omega^2 \alpha_l \Lambda_0}{\{4c_l^2 Q_{||}^2 \alpha_l \alpha_t - [(\Omega + i\eta)^2 - 2c_t^2 Q_{||}^2]^2\}}. \quad (2.25)$$

This result, when combined with relations given earlier, provides the following expression for the renormalized

force constant $\tilde{k}_0(Q_{||}, \Omega)$ which enters Eq. (2.17):

$$\frac{\tilde{k}_0(Q_{||}, \Omega)}{k_0} = \left[1 - \frac{M_A \omega_1^2}{\rho A_0} \frac{\Omega^2 \alpha_l}{[(\omega^2 - 2c_t^2 Q_{||}^2)^2 - 4c_t^4 Q_{||}^2 \alpha_l \alpha_t]} \right]^{-1}. \quad (2.26)$$

In Eq. (2.26), $\omega_1 = (k_0 / M_A)^{1/2}$ is the frequency of vibration of an isolated atom, normal to the surface, for the case where the substrate is rigid.

The expression in Eq. (2.26), combined with Eq. (2.17), is the principal result of this section. We shall discuss the consequences of coupling between the substrate and adsorbate motions in Sec. III. It is straightforward in principle to extend the treatment here to the case where the substrate is not regarded as an isotropic continuum, but as remarked earlier, when this is attempted, the complexity of the resulting algebraic expressions makes it difficult to appreciate the physical content of the results.

III. DISCUSSION AND RESULTS

We begin by sketching the consequences of the result obtained in Sec. II. Consider, for simplicity, a monolayer

$$\Omega_1^2 = \omega_1^2 \left[1 - \frac{M_A \omega_1^2 a_0^3}{\sqrt{3} M_s d_0^2} \frac{\Omega_1^2 \alpha_l}{\{[(\Omega_1 + i\eta)^2 - 2c_t^2 Q_{||}^2]^2 - 4c_t^4 Q_{||}^2 \alpha_l \alpha_t\}} \right]^{-1}. \quad (3.2)$$

In principle, at least, we are to solve Eq. (3.2) for Ω_1 . In the rigid substrate limit, Ω_1 is dispersionless, and with lateral interactions of central-force character only, the adsorbates may be regarded as a collection of Einstein oscillators insofar as their motion normal to the surface is concerned.

Quite clearly, coupling to the substrate motions induces dispersion into the perpendicular branch. The physical origin of this dispersion is indirect interactions between adsorbates induced through the dynamic response of the substrate. Dispersion of this origin has been discussed previously,¹⁰⁻¹² and is responsible for the dramatic dispersion found for the perpendicular surface phonon associated with the $c(2 \times 2)$ oxygen overlayer on Ni(100).¹² For the systems of interest here, we shall find that the substrate-induced dispersion is very modest.

Suppose we let $Q_{||} \rightarrow 0$ in Eq. (3.2). Then the term in $\alpha_l \alpha_t$ vanishes from the denominator while the factor of α_l in the numerator is replaced by $i\Omega_1 / c_l$, as $\eta \rightarrow 0$. We then have

$$\begin{aligned} \Omega_1^2 &= \omega_1^2 / \left[1 - i \frac{M_A a_0^3}{\sqrt{3} M_s d_0^2} \frac{\omega_1^2}{c_l \Omega_1} \right] \\ &\cong \omega_1^2 / \left[1 - \frac{i}{\sqrt{3}} \frac{M_A a_0^3}{M_s d_0^2} \frac{\omega_1}{c_l} \right]. \end{aligned} \quad (3.3)$$

The main point is that at $\bar{\Gamma}$ in the two-dimensional Brill-

ouin zone ($Q_{||} = 0$), the perpendicular mode frequency acquires an imaginary part, and hence a finite lifetime, even in the harmonic approximation of lattice dynamics. As the vertical motion of the adsorbate layer is excited, the substrate is dragged into motion, and the energy stored in the adsorbate layer is radiated off into the bulk of the crystal, in the form of longitudinal phonons which propagate normal to the surface. The adsorbate perpendicular mode thus becomes a "leaky" surface mode, or surface resonance, as discussed in Sec. I, and in earlier papers on other systems.^{6,10-12} As one moves away from $Q_{||} = 0$ in the present model, in the regime where $0 < Q_{||} < \omega / c_l$, both longitudinal and transverse bulk phonons are generated by the vibrating adsorbate layer, while in the regime $\omega / c_l < Q_{||} < \omega / c_t$, damping is provided only by bulk transverse modes. Finally, when $(\omega / c_t) < Q_{||}$, both α_l and α_t are real, and the only role of coupling is the introduction of dispersion into the perpendicular monolayer mode. Note, as discussed earlier,⁶ to obtain a proper description of radiation damping of the adsorbate vibrations of overlayers, it is necessary to carry out a study which employs a truly semi-infinite substrate; slab calculations¹³ show a narrow range of frequencies within which there is strong hybridization between the overlayer and standing wave bulk slab modes, but true radiation damping fails to appear.

The numerical calculations presented below show that near $\bar{\Gamma}$, the radiation damping is appreciable, for the rare-gas overlayers on Ag(111). It would thus be of very

$$\Omega_1^2 = \frac{1}{M_A} \tilde{k}(Q_{||}, \Omega_1). \quad (3.1)$$

great interest to study, possibly by high-resolution inelastic helium atom scattering, the temperature variation of the linewidth of the rare-gas overlayer phonons. Near the Brillouin-zone boundary of the overlayer, the radiation damping should be absent (in a theoretical picture such as ours which ignores umklapp processes), and the linewidth should thus be dominated by temperature-dependent anharmonic contributions. But near $\bar{\Gamma}$, in the regime $0 < Q_{||} < \omega/c_t$, the temperature-dependent anharmonic contributions should be supplemented by the temperature-independent "radiative leak" contribution displayed in Eq. (3.3). The situation will be less simple if full account of the incommensurate nature of the overlayer is taken, and careful linewidth studies may thus provide considerable insight into the interaction between an incommensurate overlayer and the underlying substrate.

In the limit $Q_{||} > \omega/c_t$ both α_l and α_t become real and, as remarked above, the substrate induces dispersion into the monolayer mode. When $Q_{||} \gg \omega/c_t$, one finds that Eq. (3.2) becomes

$$\Omega_1^2 \cong \omega_1^2 / \left[1 + \frac{M_A}{2\sqrt{3}M_s} \frac{a_0^3 c_t^2}{d^2 c_t^2} \frac{1}{(c_t^2 - c_l^2)} \frac{1}{Q_{||}} \right]. \quad (3.4)$$

Comparison of Eq. (3.2) with discussions of Rayleigh surface phonons on the semi-infinite substrate¹⁴ show that the factor $(\Omega^2 - 2c_t^2 Q_{||}^2)^2 - 4c_t^4 Q_{||}^2 \alpha_l \alpha_t$ vanishes at the Rayleigh wave frequency $\Omega = c_R Q_{||}$, where c_R is the speed of the Rayleigh wave. There is in fact strong hybridization between the monolayer mode and the Rayleigh wave where the two cross, as suggested by Fig. 1. The consequences of this hybridization will be explored in detail in the numerical calculations in the following.

To explore the influence of coupling between the adsorbate and the substrate, we have calculated the spectral density function which describe the frequency spectrum of atomic displacements normal to the surface, for atoms in the monolayer, and in the outermost layer of the bilayer and the trilayer. While we have employed such spectral density functions in earlier work,^{7,13} perhaps a brief review of their definition and physical interpretation will prove useful.

Consider the displacement $w_\alpha(I_{||} l_z; t)$ of an atom in the overlayer. We may write, for a perfectly ordered overlayer,

$$w_\alpha(I_{||}, l_z; t) = \frac{1}{(N_s)^{1/2}} \sum_{\mathbf{Q}_{||}} w_\alpha(\mathbf{Q}_{||}, l_z; t) e^{i\mathbf{Q}_{||} \cdot I_{||}}, \quad (3.5)$$

where the sum on $\mathbf{Q}_{||}$ ranges over the relevant two-dimensional Brillouin zone, and N_s is the number of unit cells in the basic two-dimensional lattice.

Quite clearly, the time variation of the $w_\alpha(\mathbf{Q}_{||}, l_z; t)$ provides us with a description of the frequency spectrum of those fluctuations with wave vector $\mathbf{Q}_{||}$, in the Cartesian direction α , and the layer labeled by l_z . For a discussion of He scattering from the rare-gas overlayer, it is the displacements normal to the surface ($\alpha = z$) in the outermost layer that are of primary importance. Thus, it is these displacements that we study along the line $\bar{\Gamma} - \bar{M}$ in the two-dimensional Brillouin zone of the hexagonal lattice.

If we describe the lattice dynamics in the harmonic ap-

proximation, then the normal modes of the adsorbate-substrate complex may be labeled by the wave vector $\mathbf{Q}_{||}$, and a second index s which designates which of the modes of wave vector $\mathbf{Q}_{||}$ (Rayleigh wave, or a particular bulk phonon, for example) we are concerned with. Then, the operator $w_\alpha(\mathbf{Q}_{||}, l_z; t)$ is related to the annihilation and creation operators $a(\mathbf{Q}_{||}, s)$, $a^\dagger(\mathbf{Q}_{||}, s)$ for the mode $(\mathbf{Q}_{||}, s)$ as follows:

$$w_\alpha(\mathbf{Q}_{||}, l_z; t) = \sum_s \left[\frac{\hbar}{2M(l_z)\omega(\mathbf{Q}_{||}, s)} \right]^{1/2} e_\alpha(\mathbf{Q}_{||}, s; l_z) \times [a(\mathbf{Q}_{||}, s) e^{-i\omega(\mathbf{Q}_{||}, s)t} + a^\dagger(\mathbf{Q}_{||}, s) e^{+i\omega(\mathbf{Q}_{||}, s)t}]. \quad (3.6)$$

Here, $e_\alpha(\mathbf{Q}_{||}, s; l_z)$ is an eigenvector normalized so that

$$\sum_\alpha \sum_{l_z} |e_\alpha(\mathbf{Q}_{||}, s; l_z)|^2 = 1,$$

$M(l_z)$ is the mass of the atoms in layer l_z , and $\omega(\mathbf{Q}_{||}, s)$ is the frequency of the mode. It is a simple matter to calculate the correlation function, to find

$$\begin{aligned} \langle w_\alpha^\dagger(\mathbf{Q}_{||}, l_z; t) w_\beta(\mathbf{Q}_{||}, l'_z; 0) \rangle_T \\ = \frac{\hbar}{2[M(l_z)M(l'_z)]^{1/2}} \int_0^\infty d\Omega \frac{1}{\Omega} [1 + 2\bar{n}(\Omega)] e^{-i\Omega t} \\ \times \rho_{\alpha\beta}(\mathbf{Q}_{||}; l_z, l'_z; \Omega), \end{aligned} \quad (3.7)$$

where $\rho_{\alpha\beta}(\mathbf{Q}_{||}; l_z, l'_z; \Omega)$ is the spectral density function, whose physical interpretation is that it provides the frequency spectrum of these fluctuations, all with wave vector $\mathbf{Q}_{||}$, which contribute to the correlation function on the left-hand side of Eq. (3.7). We have

$$\begin{aligned} \rho_{\alpha\beta}(\mathbf{Q}_{||}; l_z, l'_z; \Omega) \\ = \sum_s e_\alpha(\mathbf{Q}_{||}, s; l_z) e_\beta^*(\mathbf{Q}_{||}, s; l'_z) \delta(\Omega - \omega_s(\mathbf{Q}_{||})). \end{aligned} \quad (3.8)$$

If we choose $\alpha = \beta = z$, and $l_z = l'_z$, with l_z as the label of the outermost layer of adsorbate, then $\rho_{zz}(\mathbf{Q}_{||}; l_z, l_z; \Omega)$ describes the frequency spectrum of the atomic motions in the outermost layer, normal to the surface, and with wave vector $\mathbf{Q}_{||}$. It is this function that we compute here. One may derive a prescription for constructing this spectral density from our earlier papers.^{6,10} We first begin by writing Eq. (2.17) in the form

$$\Omega^2 w_\alpha(\mathbf{0}, l_z) - \sum_{\beta, l'_z} \tilde{d}_{\alpha\beta}(\mathbf{Q}_{||}; l_z, l'_z; \Omega) w_\alpha(\mathbf{0}, l'_z) = 0, \quad (3.9)$$

where the frequency dependence in $\tilde{d}_{\alpha\beta}(\mathbf{Q}_{||}; l_z, l'_z; \Omega)$ arises from that in the renormalized force constant $k_0(\mathbf{Q}_{||}, \Omega)$. Then, we may construct $\rho_{zz}(\mathbf{Q}_{||}; l_z, l_z; \Omega)$ by first introducing the Green's function, considered as a function of the complex frequency z ,

$$U_{\alpha\beta}(\mathbf{Q}_{||}; l_z, l'_z; z) = \sum_s \frac{e_{\alpha}(\mathbf{Q}_{||}, s; l_z) e_{\beta}^*(\mathbf{Q}_{||}, s; l'_z)}{\omega^2(\mathbf{Q}_{||}, s) - z^2}. \quad (3.10)$$

We have the following prescription:

$$\rho_{zz}(\mathbf{Q}_{||}; l_z, l'_z; \Omega) = \frac{\Omega}{i\pi} \text{Im}[U_{zz}(\mathbf{Q}_{||}; l_z, l'_z; \Omega + i\eta)], \quad (3.11)$$

where η is a positive infinitesimal quantity. Finally, one may show that the Green's function introduced into Eq. (3.10) obeys a simple inhomogeneous version of Eq. (3.9):

$$z^2 U_{\alpha\beta}(\mathbf{Q}_{||}; l_z, l'_z; z) - \sum_{\beta\gamma l''_z} \tilde{d}_{\alpha\gamma}(\mathbf{Q}_{||}; l_z, l''_z) U_{\gamma\beta}(\mathbf{Q}_{||}; l''_z, l'_z; z) = \delta_{\alpha\beta} \delta_{l_z l'_z}. \quad (3.12)$$

To calculate $U_{zz}(\mathbf{Q}_{||}; l_z, l'_z; z)$, we proceed as follows: (i) Place a factor of unity on the right-hand side of that member of Eq. (3.9) for which l_z refers to the outermost adsorbate layer, and α is z ; (ii) replace the frequency Ω by $\Omega + i\eta$. In practice, η is chosen to be a finite, small positive number equal to a few percent of the phonon frequencies of interest. (iii) Then invert the set of inhomogeneous equations, equal in number to $3n$, where n is the number of adsorbate overlayers. (iv) The element $w_z(\mathbf{0}, l_z)$ that results from this procedure is in fact $U_{zz}(\mathbf{Q}_{||}; l_z, l'_z; \Omega + i\eta)$, and the spectral density is formed from Eq. (3.11).

The simplest case is a monolayer of adsorbate atoms coupled to the rigid substrate. Then, as long as the lateral interactions have central-force character, the vibrational mode polarized normal to the surface is dispersionless, with the frequency $\omega_1 = (k_0/M)^{1/2}$ used earlier in this section. For this mode only, the adsorbates behave as a set of uncoupled Einstein oscillators. In this limit, if one traces through the definition of the spectral density, one has (with $l_z = 0$ designating the monolayer)

$$\rho_{zz}(\mathbf{Q}_{||}; 0, 0; \Omega) = \delta(\Omega - \omega_1). \quad (3.13)$$

Figure 3 shows calculations of $\rho_{zz}(\mathbf{Q}_{||}; 0, 0; \Omega)$, for several values of $\mathbf{Q}_{||}$ along the line from $\bar{\Gamma}$ to \bar{M} . The resulting force constant k_0 is chosen to reproduce the frequency $\omega_1 = 2.83$ meV for vibration of a Xe atom against the rigid Ag substrate, and lateral interactions between the adsorbed Xe atoms are modeled via Barker's gas-phase potential, with lateral interactions extended out to fifth neighbors. (This is model C of Ref. 3.) The Ag substrate is modeled as a semi-infinite isotropic elastic continuum as described in Sec. II, with elastic constants chosen to reproduce the velocity of longitudinal and transverse sound waves along the (111) direction of the real crystal. The reason for this choice is that the principal effect of coupling between the adsorbate and substrate motions will be the radiative damping of the adsorbate modes near $\bar{\Gamma}$. The bulk phonons which participate in this damping leave small values of the wave-vector component parallel to the surface, and thus propagate nearly parallel to the (111) direction. A dimensionless measure of wave vector is q , and we have $q = 1$ at \bar{M} .

At \bar{M} , we see a single feature in the spectral density at

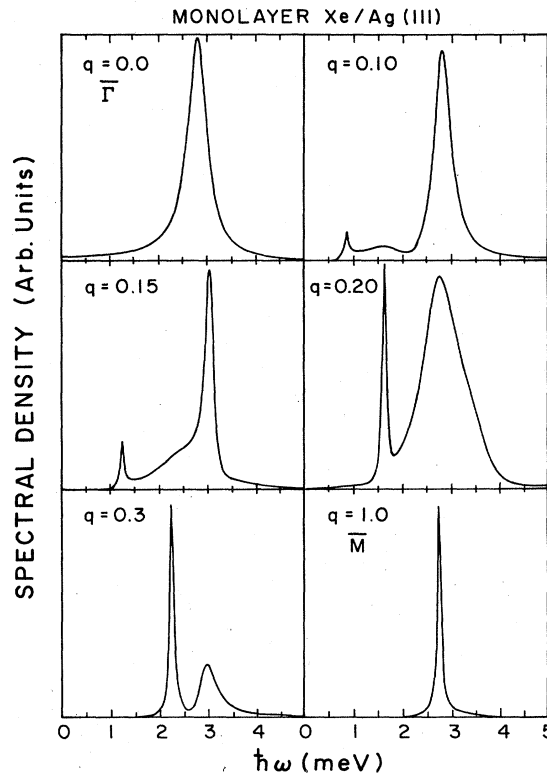


FIG. 3. Plots of the spectral density function ρ_{zz} for the xenon monolayer on a Ag(111) surface, with the Ag substrate described as a semi-infinite isotropic elastic continuum. The plots explore various wave vectors along the line from $\bar{\Gamma}$ to \bar{M} in the two-dimensional Brillouin zone of the monolayer, with dimensionless measure of the wave vector $\mathbf{Q}_{||}$. At \bar{M} , $q = 1.0$.

the frequency 2.75 meV, within the accuracy of the plot. Strictly speaking, the contribution to ρ_{zz} from this mode is a δ function, and small finite width of the feature displayed has its origin in our use of a finite value of the quantity η in Eq. (3.11). Thus, at and near \bar{M} , coupling between adsorbate and substrate motions has very little effect on the perpendicular motion.

At $\bar{\Gamma}$, where $q = 0$, we again see a single feature in the spectral density, upshifted a bit from 2.75 to 2.85 meV by coupling to the substrate vibrations. The feature at $\bar{\Gamma}$ is very much broader than that at \bar{M} , however. This linewidth has its origin in radiative damping of the perpendicular vibration mode, as discussed earlier. At \bar{M} , as suggested in Fig. 1, such radiative damping is kinematically forbidden, but it is allowed at $\bar{\Gamma}$. The linewidth in the full calculation is in reasonable accord with that provided by the expression in Eq. (3.3).

As we move out to $q = 0.1$, we see a low-frequency "wing" on the adsorbate peak. This has its origin in excitation of the adsorbate layer by bulk phonons which reflect off the substrate surface, and excite adsorbate layer motions in the process. The small peak near 0.8 meV has its origin in the substrate Rayleigh wave, with frequency given by $c_R Q_{||}$ in our model with c_R being the speed of

the Rayleigh surface wave on the substrate. As q is increased to 0.15, the Rayleigh wave increases in frequency, and by the time $q=0.20$ the Rayleigh wave on the bare substrate surface hits quite close to ω_{\perp} . The two modes thus hybridize and mix, to produce a doublet in the spectral density. The high-frequency feature, centered at 2.7 meV, contains nearly all the integrated strength, and is also broadened greatly by radiative damping. At $q=0.3$, most of the strength resides in the low-frequency feature, centered near 2.3 meV. With further increase in q , this feature very soon moves up to 2.75 meV (see Fig. 4, discussed below), and there is very little "action" in the spectral density for $0.4 < q < 1.0$, i.e., we have only a single feature very near 2.75 meV.

We then see from this example the principal effects of coupling between adsorbate and substrate motions. Near $\bar{\Gamma}$, we have substantial "radiative damping" of the adsorbate normal mode, and there is hybridization between the Rayleigh wave and the monolayer mode that produces a doublet in the spectral density; the two features in the doublet have comparable intensity only quite near the crossover between the substrate Rayleigh wave, and the dispersionless vibrational mode of the adsorbate overlayer.

In Fig. 4, we plot the trajectories of the structures which appear in the spectral density. The solid line is the frequency of the dispersionless mode of the monolayer vibrating normal to a rigid substrate. Solid circles give the frequency of the Rayleigh surface wave of the substrate with adsorbate layer absent. These points are provided by a slab calculation, discussed below, and serve as a check of our modeling of the substrate as an elastic continuum. Over the region of the two-dimensional Brillouin zone appropriate to the present analysis, the slab calculation shows the substrate Rayleigh mode to be quite dispersionless. The triangles represent the location of the peaks in ρ_{zz} , calculated as displayed in Fig. 3. Keep in mind that

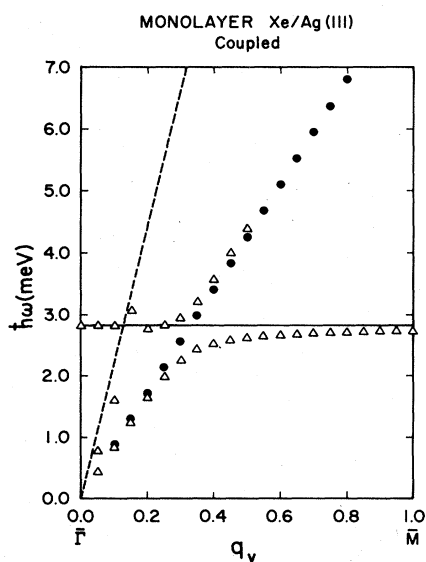


FIG. 4. Trajectories of peaks in the spectral density ρ_{zz} in the ω - Q_{\parallel} plane, for the xenon overlayer on Ag(111).

away from the Rayleigh wave-adsorbate mode crossover, one member of the doublet has very modest integrated strength. We see the hybridization phenomenon very clearly here. Note the smaller degree of anomalous dispersion introduced when the adsorbate mode crosses the line $\omega=c_l Q_{\parallel}$, with c_l the longitudinal-phonon sound velocity. There is a Van Hove singularity of the form $(\omega-c_l Q_{\parallel})^{-1/2}$ in the projected density of states of the bulk phonons which produce this anomaly.

We turn next to a discussion of the second model, which places a hexagonal xenon overlayer over a Ag(111) crystal, modeled as a finite slab of silver layers. It has been pointed out by Unguris *et al.*² that the lattice constant of the xenon overlayer is close to 1.5 that of the underlying silver substrate, although in fact the two lattices are actually incommensurate. If we use the lattice constant of the monolayer reported in Ref. 3, 4.38 Å, then the lattice constant ratio is 1.516. For the xenon bilayer, the ratio is 1.4965. Thus, in our model, we make the two commensurate by choosing the ratio to be precisely $\frac{3}{2}$.

We then have to make a decision about the manner in which the xenon overlayer is placed above the silver substrate, and we have chosen the geometry illustrated in Fig. 5. One adsorbate in each unit cell resides in a top site, and three in a twofold bridge site. The two-dimensional unit cell contains four adsorbate atoms, and nine Ag atoms. For this structure, the line from $\bar{\Gamma}$ to \bar{M} is one-third the length of the line appropriate to that in the Brillouin zone of an isolated layer of substrate atoms, and one-half of that appropriate to the adsorbate layer taken alone. One must keep these relationships in mind as we interpret the normal modes of the system.

Our calculations are carried out for the adsorbate layer placed on an eight layer slab of the Ag atoms. We use a nearest-neighbor model for the lattice dynamics of the structure, with the single bulk force constant chosen to reproduce the maximum bulk phonon frequency of silver, and each xenon is coupled to the substrate by force constants adjusted so each of the force atoms in the unit cell has the same perpendicular vibration frequency, with substrate atoms held pinned in place.

We calculate all of the normal modes of the above structure, and calculate $\bar{e}_1^2 = \frac{1}{4} \sum_{i=1}^4 |e_z^{(i)}|^2$ for each of

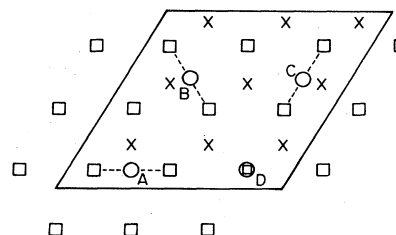


FIG. 5. The geometry chosen for placement of the xenon overlayer on the Ag(111) surface. The circles are xenon adsorbates, the squares are the outermost layer of Ag atoms, and the crosses denote the location of the atoms in the second layer down. The four inequivalent adsorbate atoms in the unit cell (parallelogram) are designated A, B, C, and D.

these, where $e_z^{(i)}$ is the z component of motion of the i th atom in the xenon unit cell. We find, for most choices of wave vector parallel to the surface, four modes which contribute e_1^2 strongly enough to be detected in helium scattering measurements. The remaining modes involve primarily parallel motions of the adsorbates (8 modes), or primarily motion of substrate atoms ($8 \times 9 \times 3$ modes), although as we shall see, these are on occasion additional modes which contribute to e_1^2 significantly.

Two of the modes of interest have simple properties. One mode involves atoms B and C ; the frequency shifts from 2.70 meV at the zone center to the slightly downshifted value 2.69 meV at the zone boundary of the unit cell of the structure in Fig. 5. The other involves almost exclusively atom A , and its frequency varies from 2.70 to 2.68 meV in the same sweep through the zone. Both these modes have 99% of the motion stored in the atoms described above, with $|e_z|^2$ as a measure.

In Fig. 6, we compare the spectral density functions ρ_{zz} generated by the model which treats the substrate as an elastic continuum, and the frequency distribution of the modes which contribute to e_1^2 , and the value of the latter

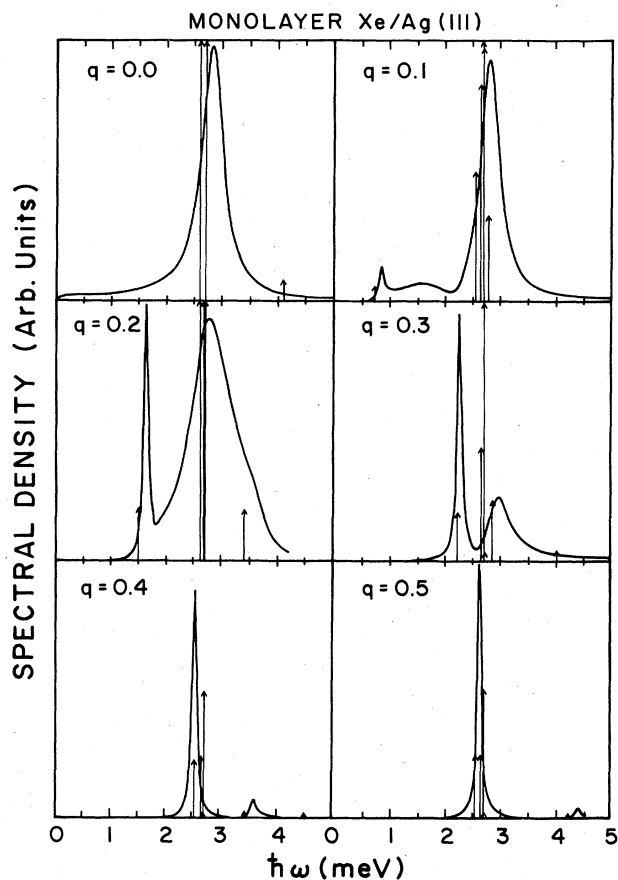


FIG. 6. Plots of the spectral density functions ρ_{zz} generated by the model which treats the substrate as an elastic continuum (solid lines), and a comparison with the spectral distribution of e_1^2 generated from the slab calculation.

quantity. The two sets of calculations track remarkably well, along the portion of the line from $\bar{\Gamma}$ to \bar{M} explored here. The slab calculation leads to a slightly smaller hybridization gap at $q=0.3$, and places more weight in the high-frequency members of the doublet than the continuum model. The slab calculations thus provide support for the predictions of the continuum model, although our past experience suggests that the substrate has not been taken thick enough for us to have confidence that convergence has been achieved fully. For eight silver layers, to obtain these results we had to diagonalize a 228×228 matrix (size $8 \times 9 \times 3 + 4 \times 3$); each new substrate layer increases the size of the matrix by 27 rows and columns, and we could not handle a larger slab with the machine available to us (Burroughs 7900). However, it is quite clear that our continuum model and the second model which takes account of the discrete atomic structure of the substrate produce very similar results.

We now turn to our results for the xenon bilayer and xenon trilayer, with the silver substrate described within the framework of the isotropic elastic continuum model. For these calculations, the xenon bilayer and the trilayer are described by model C of Ref. 3, i.e., we have lateral interactions described through the use of Barker's potential, summed out to fifth neighbors.

In Fig. 7(a) we show those phonon branches, four in number, which are polarized with displacement in the sagittal plane which contains the normal to the surface, and the line from $\bar{\Gamma}$ to \bar{M} . These are calculated for the bilayer

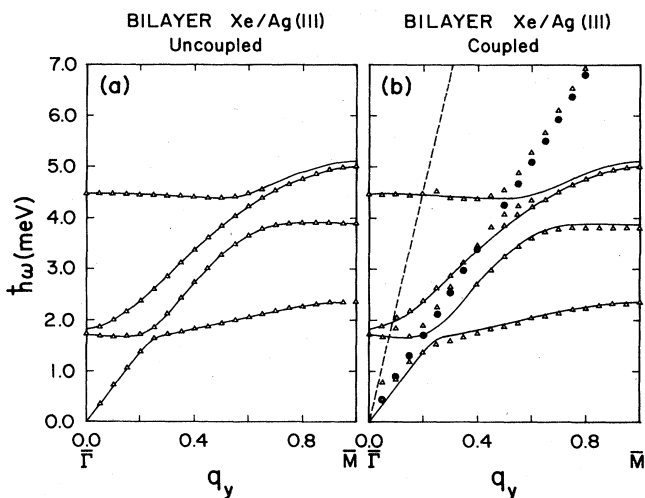


FIG. 7. (a) The dispersion curves, along the $\bar{\Gamma}-\bar{M}$ line, for those phonons of the xenon bilayer with displacement in the sagittal plane. The solid lines are calculated by diagonalizing the appropriate dynamical matrix, while the triangles denote the position of the peaks in ρ_{zz} . The portions of the dispersion curve with no triangles are regions where the mode contributes very little to the perpendicular motions of atoms in the outer layer. (b) The trajectories of the peaks in ρ_{zz} in the $\omega-Q_{\parallel}$ plane of the peaks in the spectral density for vertical motion of atoms in the outermost layer. Superimposed is the dispersion relation of the substrate Rayleigh wave (solid circles), the line $\omega = c_l Q_{\parallel}$ (dashed line), and the rigid substrate bilayer dispersion curves (solid lines).

which vibrates on a rigid substrate. For simplicity, we omit the two shear horizontal branches, with polarization parallel to the surface and normal to the sagittal plane. The solid lines are calculations of the dispersion curves, found by diagonalizing the problem defined by Eq. (2.14) with zero on the right-hand side, and the triangles show the positions of the peaks in ρ_{zz} , again with the substrate held rigid. This comparison serves as a check on our computational procedures. Figure 7(b) shows the trajectories of the peaks in ρ_{zz} , with coupling to the substrate included. The solid circles give the dispersion relation for the substrate Rayleigh wave, with adsorbate bilayer absent, while triangles give the trajectories of the peaks in ρ_{zz} . The shifts in frequency away from the rigid substrate bilayer phonon bands is small, through most of the Brillouin zone save near the crossover of the Rayleigh wave with the various branches. In these regions of the plot, extra structures appear.

In Figs. 8 and 9, for various values of the reduced wave vector along the $\bar{\Gamma}-\bar{M}$ line, we show plots of ρ_{zz} for the outer layer of the bilayer. For each value of q , we show the calculation which incorporates substrate motions in the left-hand column while the right-hand column displays ρ_{zz} in the limit of a rigid substrate. At $q=0$, we see two features in the spectral density; the role of radiative damping is evident when the two are compared. For

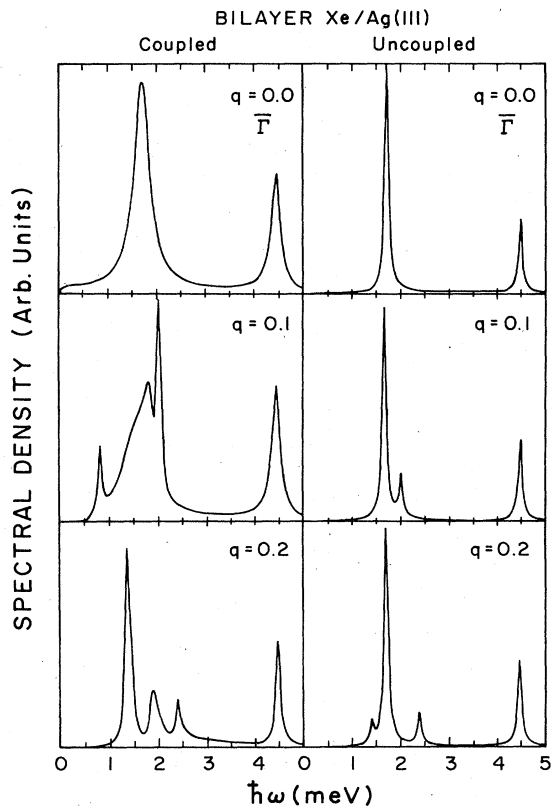


FIG. 8. For values of $0 \leq q \leq 0.2$, we show ρ_{zz} for the case where the bilayer is coupled to the substrate motions (left-hand column of the figure) and for the case where the substrate is assumed rigid.

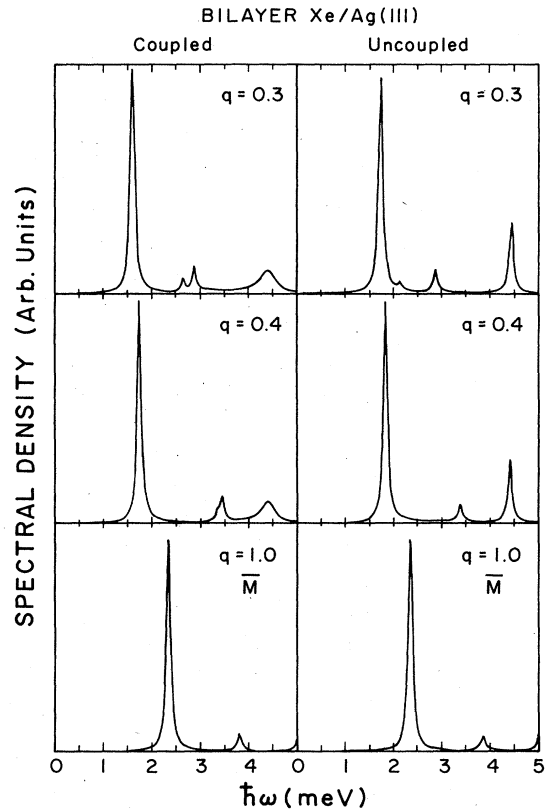


FIG. 9. Same as Fig. 8 but now for $q=0.3, 0.4$, and 1.0 .

$q=0.1$, in the right-hand column, we see a doublet, which shows that each of the two branches in Fig. 7(a) contribute to ρ_{zz} in the rigid substrate limit, although the higher frequency member of the pair is a weak feature. At this value of q , with coupling to the substrate "turned on," the feature near 0.7 meV is produced by the substrate Rayleigh wave. The doublet between 1.5 and 2.0 meV is distorted, with redistribution of oscillator strength between the two modes, by the near proximity of this feature to the Van Hove singularity associated with the "longitudinal edge" at $\omega=c_l Q_{||}$. In essence, there is appreciable coupling here between the bilayer modes, and bulk longitudinal phonons which propagate nearly perpendicular to the surface.

For this system, the Rayleigh wave velocity nearly coincides with that of the low-frequency acoustical phonon of the bilayer, so this pair couples to produce only a single feature in the spectral density. There is, in principle, a hybridization splitting, but evidently for q near zero, this is smaller than the linewidth produced by radiative broadening. Thus, at $q=0.2$, below 2.5 meV, we see only three spectral features as in the rigid substrate calculation but the mode mixing produces a substantial redistribution of oscillator strength.

For values of the reduced wave vector q equal to or greater than 0.3, the coupling between the adsorbate and substrate motions produces no dramatic effects on the dominant feature in the spectral density, although surely the details in ρ_{zz} are affected. Our conclusions are that

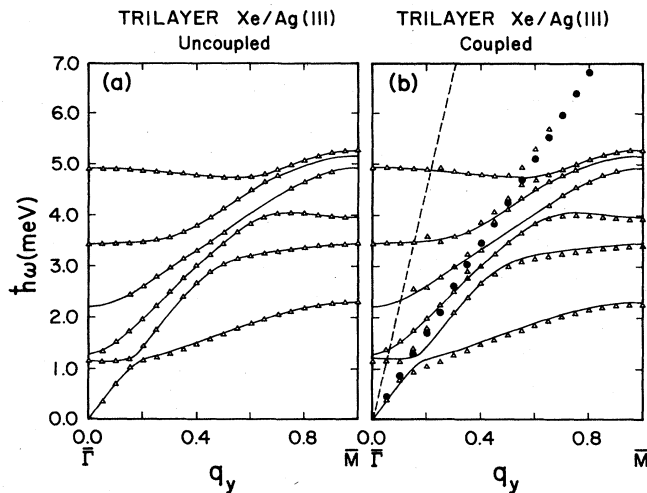


FIG. 10. In parts (a) and (b) we give information similar to that provided by Fig. 7, but for a xenon trilayer coupled to a semi-infinite Ag substrate, modeled as an elastic continuum.

for the bilayer, the influence of coupling between adsorbate and substrate motions is confined to the near vicinity of $\bar{\Gamma}$ ($q \leq 0.25$) where, alas, high resolution data can be hard to obtain.

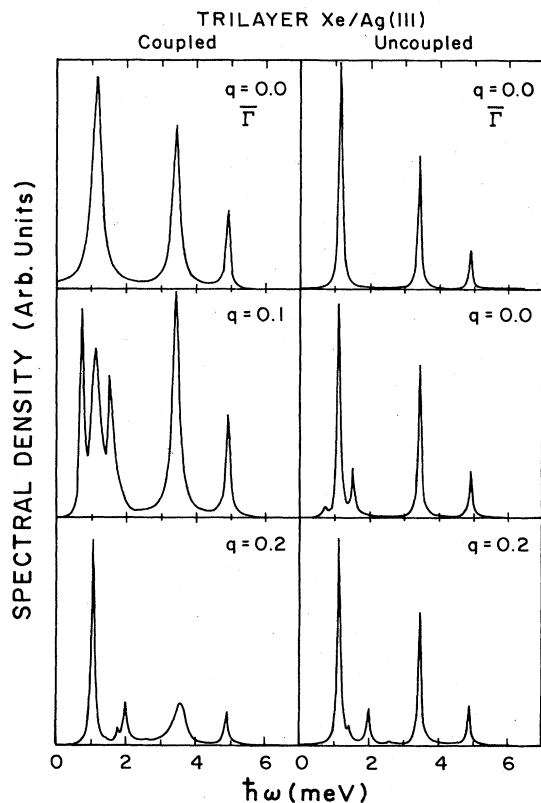


FIG. 11. Same as Fig. 8 but for the trilayer rather than the bilayer.

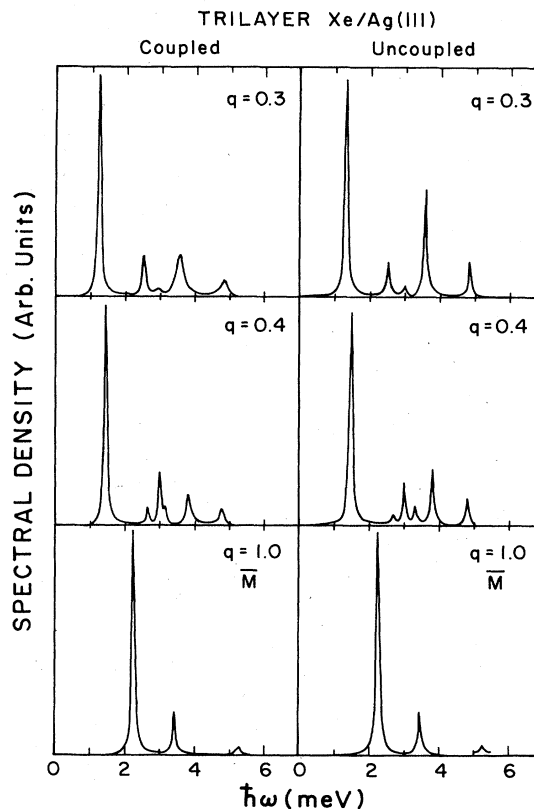


FIG. 12. Same as Fig. 9 but for the trilayer rather than the bilayer.

We now turn to the trilayer. In Fig. 10(a) we give the dispersion curves of the trilayer phonon modes with displacement in the sagittal plane, while Fig. 10(b) gives the trajectories of peaks in ρ_{zz} . Then Figs. 11 and 12 provide plots of ρ_{zz} , for the case where the trilayer is coupled to the substrate motions (left-hand column), and where it vibrates on a rigid substrate. At $\bar{\Gamma}$, we see the influence of radiative damping of the adsorbate modes, but the effect is less dramatic than in the case of the monolayer and the bilayer. Mixing between the Rayleigh wave and the overlayer vibrations produces dramatic enhancements in the spectral strength of the low-frequency features near 1 meV for $q=0.1$, but by the time $q=0.2$, the influence of coupling is only on minor features in ρ_{zz} . This remains true for all larger values of q .

From a comparison between the monolayer, bilayer, and trilayer results, it is evident that as the layer thickness increases, the influence of coupling between adsorbate and substrate motions is dramatic in a progressively smaller fraction of the Brillouin zone near $\bar{\Gamma}$. We assume the reason is that as $Q_{||}$ increases, the displacements in the Rayleigh wave become more and more localized to the overlayer-substrate interface, and when this degree of localization is small compared to the overlayer thickness, the substrate Rayleigh wave has little influence on the dynamical properties of the outermost layer. Thus, as more layers are added to the adsorbate complex, the influence of the substrate becomes progressively more localized to the near neighborhood of $\bar{\Gamma}$.

IV. CONCLUDING REMARKS

The principle conclusions that follow from this study, and their consequences are as follows.

(i) The frequency shifts produced by coupling between substrate and adsorbate motions are rather small throughout much of the two-dimensional Brillouin zone, except for regimes of wave vector where the substrate Rayleigh wave dispersion curve crosses a branch of a mode localized by the adsorbate layer, with symmetry such that its displacement is confined to the sagittal plane. Then, rather dramatic hybridization splittings can occur, particularly for the monolayer. Less dramatic but nonetheless clear anomalous dispersion is introduced when adsorbate layer dispersion curves cross the line $\omega = c_t Q_{||}$; this has its origin in a Van Hove singularity in the projected bulk phonon densities of states.

We believe that substrate-induced anomalous dispersion should be observable in inelastic He atom scattering experiments, carried out with very high resolution. When examining our spectral density plots, the reader must keep in mind that they explore the frequency spectrum of atom motions in the outermost adsorbate layer associated with a particular wave vector $Q_{||}$. In an actual experiment, with incident-beam direction fixed, and detector fixed, one samples a range of $Q_{||}$ values in the study of the loss spectrum.

(ii) Radiative damping, in which adsorbate modes decay by emitting their energy into the substrate in the form of bulk phonons, can be strong in those regions of the two dimensional Brillouin zone where these processes are kinematically allowed (see Fig. 1). The adsorbate modes are damped quite strongly by this process, according to our calculations. It would be intriguing to study the temperature variation of the linewidth of the monolayer perpendicular mode as a function of its wave vector $Q_{||}$. Near \bar{M} , where the frequency ω is small compared to $c_t Q_{||}$ and $c_l Q_{||}$, radiation damping is not allowed kinematically, so anharmonicity is the only source of linewidth. This latter contribution should exhibit a clear temperature dependence, similar to that expected for the higher frequency adsorbate normal modes of chemisorbed atoms.¹⁵ Near $\bar{\Gamma}$, where the radiative damping is allowed, there should be substantial temperature-independent contribution to the linewidth, with origin in the radiative damping.

It must be kept in mind that the kinematical conditions cited here for the occurrence of radiation damping will be modified, if due account is taken of the incommensurate nature of the overlayer. In effect, umklapp processes not included in the present treatment are possible kinematically. We suspect these are weak, because of the very smooth nature of the Ag(111) surface, but their presence and possible study may provide insight into the role of incommensurability in surface lattice dynamics, for systems such as those studied here.

(iii) The influence of interaction between the substrate motions and those in the overlayer are most pronounced for the monolayer, and as one moves to the bilayer and the trilayer, the influence of the coupling is confined to a smaller and smaller fraction of the Brillouin zone, near $\bar{\Gamma}$.

The monolayer should thus be the system to be studied first to search for such an effect, with the present calculations and discussion as a guide.

We conclude with some general remarks on a comparison between the information provided by our analysis of the adsorbate layer placed on a semi-infinite substrate, and the studies based on the slab method. As noted earlier, de Wette and his colleagues have carried out detailed studies of Kr overlayers¹³ or graphite, which are commensurate with the underlying substrate, modeling the substrate by a finite slab substantially thicker than that employed here. In principle, a proper description of radiation damping appears in the theory only in the limit that the substrate becomes infinitely thick, and the density of substrate phonon modes with fixed $Q_{||}$ becomes a true continuum. For a substrate slab of finite thickness, one has a discrete spectrum of substrate modes associated with each value of $Q_{||}$. In the work of Ref. 13, one sees the adsorbate branch merge with the discrete substrate mode spectrum, and the result is a spectral region within which there is strong mixing between the adsorbate modes, and the substrate mode spectrum. de Wette *et al.* comment that there is enhanced amplitude at the surface in this spectral region.

There is a direct analogy between the description of the radiative decay of an excited atom in free space, where the excited state acquires a finite lifetime by emitting photons, and coupling of an atom to the radiation field in a finite cavity with discrete modes. In the latter case, all normal modes have infinite lifetime, and there will be a spectral region within which one encounters strong coupling of the atom to the radiation field, resulting in modes of mixed character.

In earlier work, we have developed a Green's-function method that may be applied to a semi-infinite discrete lattice of substrate atoms, with^{6,10} or without¹⁶ ordered adsorbate layers. In this series of papers, we have presented detailed studies of various resonance modes, within the framework of a method which provides an *exact* description of the response of a semi-infinite substrate in the harmonic approximation. We have compared these exact results with finite slab simulations; the slab calculations produce a poor description of the width of the surface resonance, largely because with the number of layers typically included (20 to 30), only a small number of normal modes of the slab lie within the narrow spectral region where the resonance is found in the full solution. In some cases, the slab method fails to show the surface resonance mode (this can occur if a resonance lies in a spectral region where the density of bulk modes is small), or statistical fluctuations in the computational data may produce features in the spectral density that can be misidentified as resonance modes. An example of the latter problem is to be found in work published by Andersson, Karlsson, and Persson,¹⁷ who studied surface resonance modes induced by the $p(2 \times 2)$ oxygen overlayer adsorbed on a Ni(100). They identify three resonance modes from their slab calculation. In earlier work,¹⁸ precisely the same model employed by these authors was introduced to describe these systems. The exact solution presented there, with semi-infinite substrate shows that only two

and not three surface resonances are contained in the model.

For the reasons cited above, we believe the Green's function method we have developed is a superior method of describing surface resonances. With modern computers with large storage capacity, it is possible to consider much thicker slabs, with perhaps 100 substrate layers included. Then the slab results may prove more reliable, and convergence of the spectral density calculations may be checked explicitly. As we have discussed, this paper has

utilized a continuum model of the substrate, to simplify the description of the interaction between the substrate and the incommensurate overlayers of interest here.

ACKNOWLEDGMENTS

This research was supported by the U.S. Department of Energy, through Grant No. DE-FG03-84ER45083, and by the Natural Sciences and Engineering Research Council of Canada.

¹See the discussions by A. D. Novaco and J. P. McTague, *Phys. Rev. Lett.* **38**, 1286 (1977) and J. P. McTague and A. D. Novaco, *Phys. Rev. B* **19**, 5299 (1979).

²See J. Unguris, L. W. Bruch, E. R. Moog, and M. B. Webb, *Surf. Sci.* **87**, 415 (1979); P. I. Cohen, J. Unguris, and M. B. Webb, *ibid.* **58**, 429 (1976); L. W. Bruch, P. I. Cohen, and M. B. Webb, *ibid.* **59**, 1 (1976); and L. W. Bruch and J. M. Phillips, *ibid.* **91**, 1 (1980).

³Kevin Gibson, S. Sibener, Burl M. Hall, D. L. Mills, and J. E. Black, *J. Chem. Phys.* (to be published).

⁴B. F. Mason and B. R. Williams, *Phys. Rev. Lett.* **46**, 1138 (1981).

⁵Of course, even in a cubic crystal, the bulk phonons are purely transverse or longitudinal only for propagation along high-symmetry direction, therefore, this language is a bit oversimplified.

⁶A discussion of the nature and origin of surface resonance modes in a rather different physical system has been given by Talat S. Rahman, D. L. Mills, and J. E. Black, *Phys. Rev. B* **27**, 4059 (1983).

⁷B. F. Mason and B. R. Williams, *Surf. Sci.* **139**, 173 (1984).

⁸See the discussion that begins on p. 10 of L. D. Landau and E. M. Lifschitz, *Theory of Elasticity* (Pergamon, New York, 1959).

⁹G. Vidali, M. W. Cole, and J. R. Klein, *Phys. Rev. B* **28**, 3064 (1983).

¹⁰Talat S. Rahman, J. E. Black, and D. L. Mills, *Phys. Rev. B* **25**, 883 (1982); Talat S. Rahman, D. L. Mills, J. E. Black, J. M. Szeftel, S. Lehwald, and H. Lehwald, *Phys. Rev. B* **30**, 589 (1984).

¹¹Substrate-induced dispersion in adsorbate mode phonon spectra has been discussed in Chap. 5 of H. Ibach and D. L. Mills, *Electron Energy Loss and Surface Vibrations* (Academic, San Francisco, 1982).

¹²See discussion of the high frequency, perpendicularly polarized adsorbate mode found for the $c(2 \times 2)$ oxygen overlayer on the Ni(100) surface. This is discussed in the second paper cited in Ref. 10 of this paper. Also see J. M. Szeftel, S. Lehwald, H. Ibach, Talat S. Rahman, and D. L. Mills, *Phys. Rev. Lett.* **50**, 518 (1983).

¹³E. de Rouffignac, G. P. Alldredge, and F. W. de Wette, *Phys. Rev. B* **24**, 6050 (1981); F. W. de Wette, B. Firey, E. de Rouffignac, and G. P. Alldredge, *ibid.* **28**, 4744 (1983).

¹⁴See pp. 109–113 of L. D. Landau and E. M. Lifshitz, *Theory of Elasticity* (Pergamon, New York, 1959).

¹⁵J. C. Ariyasu, D. L. Mills, J. C. Hemminger, and Kathryn Lloyd, *Phys. Rev. B* **30**, 507 (1984).

¹⁶J. E. Black, Talat S. Rahman, and D. L. Mills, *Phys. Rev. B* **27**, 4072 (1983).

¹⁷S. Andersson, P. A. Karlsson, and M. Persson, *Phys. Rev. Lett.* **51**, 2378 (1983).

¹⁸See Rahman, Black, and Mills, Ref. 10.